Plasma activation of microplates optimised for one-step reagent-free immobilisation of DNA and protein

Kanako Coffi Dit Gleize,[†] Clara T. H. Tran,[*,‡] Anna Waterhouse, [*,¶,§,k,⊥] Marcela M. M. Bilek,[#,‡,k,⊥] and Shelley F. J. Wickham[*,†,‡,k]

†School of Chemistry, The University of Sydney, Sydney, NSW 2006, Australia

‡School of Physics, The University of Sydney, Sydney, NSW 2006, Australia

¶School of Medical Sciences, The University of Sydney, Sydney, NSW 2006, Australia

§The Heart Research Institute, The University of Sydney, Newtown 2042, Australia

k The University of Sydney Nano Institute, The University of Sydney, Sydney, NSW 2006, Australia

⊥Charles Perkins Centre, The University of Sydney, Sydney, NSW 2006, Australia
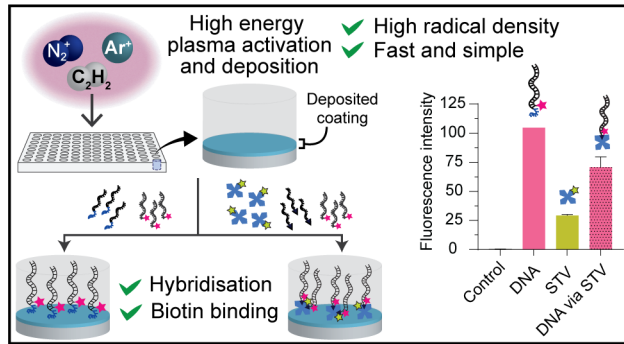
#School of Biomedical Engineering, Faculty of Engineering, The University of Sydney, NSW 2006, Australia

E-mail: clara.tran@sydney.edu.au; anna.waterhouse@sydney.edu.au; shelley.wickham@sydney.edu.au;

Phone: +61 2 9351 3366

Abstract

Activated microplates are widely used in biological assays and cell culture to immobilise biomolecules, either through passive physical adsorption or covalent cross-linking. Covalent attachment gives greater stability in complex biological mixtures. However, current multistep chemical activation methods add complexity and cost, require specific functional groups, and can introduce cytotoxic chemicals that affect downstream cellular applications. Here, we show a method for one-step linker-free activation of microplates by high energy plasma for covalent immobilisation of DNA and protein. Two types of high energy plasma treatment were shown to be effective: plasma immersion ion implantation (PIII) and plasma activated coating (PAC). This is the first time that PIII and PAC have been reported in microwell plates with non-flat geometry. We confirm that the plasma treatment generates radical-activated surfaces at the bottom of wells despite potential shadowing from the walls. Comprehensive surface characterisation studies were used to compare PIII and PAC microplate surface composition, wettability, radical density, optical properties, stability, and biomolecule immobilisation density. PAC plates were found to have more nitrogen and lower radical density and were more hydrophobic and more stable over 3 months than PIII plates. Optimal conditions were obtained for high density DNA (PAC, 0% or 21% nitrogen, pH 3-4) and streptavidin (PAC, 21% nitrogen, pH 5-7) binding, while retaining optical properties required for typical high-throughput biochemical microplate assays, such as low autofluorescence and high transparency. DNA hybridisation and protein activity of immobilised molecules were confirmed. We show that PAC activation allows for high density covalent immobilisation of functional DNA and protein in a single step on both 96 and 384 well plates, without specific linker chemistry. These microplates could be used in the future to bind other user selected ligands in a wide range of applications, for example for solid phase PCR and stem cell culture and differentiation.

High energy plasma activation and deposition

✓ High radical density
✓ Fast and simple

Deposited coating

✓ Hybridisation
✓ Biotin binding

Fluorescence intensity

Control DNA STV DNA via STV

Introduction

Microplates are a critical and ubiquitous platform for high-throughput biological assays and cell culture.[1] Applications include enzyme-linked immunosorbent assays (ELISA),[2,3] biomolecule interaction studies[4] and cell-drug interaction screening.[5] The standardised microplate format facilitates rapid optical characterisation and automation. Microplates are typically made of polystyrene, which has good optical properties but is hydrophobic and does not adhere to cells or biomolecules well. Modified plates, known as tissue culture treated plates, are treated with oxygen plasma to reduce hydrophobicity and enhance cell adhesion.[6] However, this basic tissue culture oxygen treatment is not sufficient for a growing range of techniques where high stability and density biomolecule surface immobilisation is required. For example, collagen type I coated plates can be used to isolate muscle-derived stem cells,[7] while culture on E-cadherin coated plates can maintain embryonic stem cells in a pluripotent state.[8] A limited range of chemically functionalised microplates are commercially available, but require multi-step attachment methods, lack flexibility of functional groups, and are expensive. Commercial protein coated microplates are similarly expensive, and only available for a limited range of extracellular matrix proteins. Here, we develop new methods for plasma activation of polystyrene microplates using plasma immersion ion implantation (PIII) and plasma activated coating (PAC). This is the first report of PIII or PAC on non-flat polystyrene geometries such as microplates. We show that PIII and PAC allow for simple high-density high-stability immobilisation of multiple types of biomolecules on microplates for a wide range of bioassays and cell culture applications at low cost.

Surface immobilisation of biomolecules on a solid support can be achieved via physical adsorption or covalent binding. Physical adsorption is commonly used to attach biomolecules such as DNA and proteins to microplate surfaces through hydrophobic or electrostatic interactions. Although the technique is simple, physically adsorbed

biomolecules bind weakly with random orientation[9] and are sensitive to changes in ionic concentration, pH, heat and detergent, reducing reproducibility.[10] Proteins can also be denatured by physical adsorption, for example, reducing monoclonal antibody activity to less than 10%.[11] For DNA, physical adsorption methods are unsuitable for applications in biosensing as they do not control the molecule orientation on the surface[12]

Stronger, more specific binding can be achieved through covalent immobilisation via chemical activation of microplates,[9] increasing stability, activity, and resistance to washing, and reducing competitive protein exchange from the Vroman effect.[13] Silane chemistry, for example aminopropyltriethoxylsilane (APTES), is often used for activation of surfaces for biomolecule binding.[14] This surface activation approach has been used in DNA microarrays where the DNA is functionalised with thiol or amine groups prior to chemical coupling to the surface.[10,15–17] The hybridised DNA density of such surfaces can range from 4.0×10^{10} to 6.0×10^{12} molecules/cm^2 (Table 1), while a denser hybridised DNA surface has been made by co-polymerisation using acrylamide (1.6×10^{13} molecules/cm^2).[18] Microplate surfaces have also been previously functionalised with chitosan,[19] thiol groups,[20] or primary amine groups[21,22] for protein, enzyme, peptide and *E. coli* immobilisation. However, chemical activation methods are multi-step processes, often requiring modified biomolecules such as amine-modified or thiol-modified DNA oligonucleotides, and may involve cytotoxic reagents that generate chemical waste and must be completely removed from the surface before downstream applications in cell culture.[23]

Table 1: Chemical activation methods for covalent immobilisation of DNA and corresponding DNA hybridisation densities. The substrates used in these examples are not polystyrene and have not been applied on microplates.

Surface modification	Attachment chemistry	Substrate type	Hybridisation density (molecules/cm^2)
NHS-silane[10]	Amine-DNA	Silicon wafer	4.0 x 10^{10}
Aminosilane[15]	Crosslinked via SMPB	Fused silica, silicon wafer	8.4 x 10^{10}
3-mercaptopropylsilane[16]	Disulfide-DNA	Glass slide	4.5 x 10^{12}
Aminosilane[17]	crosslinked via SIAB	Silicon wafer	6.0 x 10^{12}
Polymerisable acrylic silane[18]	Photochemical copolymerisation with acrylamide	Silica optical fibre	1.6 x 10^{13}

Covalent immobilisation of biomolecules in one step without chemical linkers is possible through radical-rich surfaces obtained from high energy plasma activation.[24] The physical treatment using the bombardment of energetic ions is fast, reproducible and the reactivity of these surfaces is retained for long periods.[25] One method to activate polymers is known as plasma immersion ion implantation (PIII) in which ions from non-carbon containing gases such as nitrogen, argon or helium are accelerated under a high electric field to bombard polymer surfaces, producing a reservoir of radicals in the sub-surface of the polymer (Figure 1a).[26] Another plasma activation method which can be used for more diverse substrates (polymers, metals, semiconductors, ceramics or glass) is plasma-enhanced chemical vapour deposition (PECVD) combined with ion bombardment induced by substrate bias.[27] In this method, a mixture of gases including a carbon-containing gas is used to generate a plasma activated coating (PAC) on the substrate surface.[24] Both PIII and PAC treated surfaces are rich in radicals which can form covalent bonds with biomolecules upon their contact with the surface. Proteins immobilised on PIII and PAC surfaces can form a dense monolayer and their activity is retained.[26,28,29] Furthermore,

DNA immobilised on PIII treated polystyrene surfaces has been shown to hybridise with its complementary sequence strand.[30] However, PIII and PAC treatment of microplates has not been reported. Additionally, DNA immobilisation on PAC surfaces has not been studied and PIII and PAC surfaces have not been directly compared for their surface properties and efficiency of biomolecule immobilisation.

While PIII and PAC treatments have been demonstrated on flat substrates such as polymer sheets,[28,31] stainless steel[29,32] and glass coverslips,[26] the effectiveness of these treatments on deep well structures such as microplates has not been explored. The deep walls of microplates have the potential to cause shadowing, preventing effective PIII or PAC treatment of the well bottom. Existing plasma treatment strategies used to immobilise biomolecules on polystyrene microplates have drawbacks. For example, argon plasma activation has been used as a pre-treatment for silane functionalisation,[33] and nitrogen plasma activation has been used to introduce amine groups for functionalisation with glutaraldehyde and other linkers.[34] However, these methods require further chemical activation steps and specific functional groups on the biomolecules. The density of active groups incorporated during plasma treatment in these approaches is also limited by gas mixtures required to produce a mechanically robust surface coating. Another approach involves the direct deposition of nebulized protein, such as collagen, on microplates by dielectric barrier discharge plasma.[35] However, this method requires large quantities of protein and not all biomolecules incorporated into the coating are accessible on the surface. PIII and PAC treatments for direct activation of microplates for biomolecule immobilisation have the potential to mitigate these limitations.

In this study, we demonstrated PIII and PAC treatments activating 96-well polystyrene microplates for the immobilisation of single-stranded DNA (ssDNA) and the protein streptavidin (Figure 1c). We select DNA to optimise the density and orientation of the

immobilised molecules to achieve high hybridisation densities.[9,36] Streptavidin is selected because it provides a generic linker for capture of any biotinylated molecule, including antibodies.[37] In addition, although the mechanisms of covalent binding of biomolecules in both PIII and PAC methods are based on the presence of radicals, each of these plasma activation techniques changes the physical and chemical properties of the substrates differently. These surface chemistry differences can potentially influence the density and orientation of adsorbed biomolecules on the surface prior to covalent bond formation. For the first time, we conducted a comprehensive comparison of the changes in optical properties, physical properties and surface chemistry of microplates treated with different PAC recipes and PIII treatments. We then compared biomolecule immobilisation on PAC and PIII to establish optimal protocols for DNA and streptavidin coated microplates and explored potential mechanisms behind covalent bond formation. Finally, we characterised the stability of PIII and PAC treated plates over 3 months. The results presented here demonstrate the potential of PIII and PAC treated microplates for a wide range of biological and biomedical assays and diagnostics.
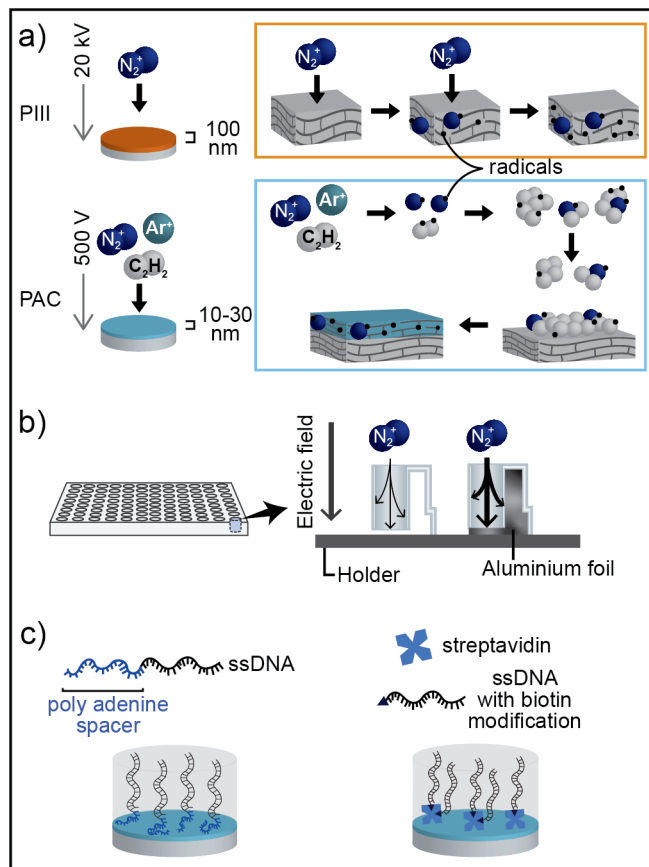
Figure 1: (a) Schematic of PIII and PAC treatment. b) Microplate on the sample holder and addition of aluminium foil to improve conduction to the bottom of the microplate wells. c) Immobilisation of ssDNA and streptavidin to PIII and PAC treated microplates.

Experimental

Microplate preparation

Most commercially available microplates are tissue culture (TC) treated which is often described as some sort of a plasma treatment.[6] In this study, high energy plasma treatment was performed on TC treated polystyrene (PS) microplates (CLS3603) (Sigma-Aldrich) and was compared to unmodified TC treated PS microplates and untreated (UT) PS microplates (CLS3370). These microplates have wells with diameter approximately 6 mm and depth approximately 11 mm. There is a 2-3 mm gap between the holder and the bottom of the well when the microplate is placed on either a PIII or a PAC stainless steel holder. Aluminium foil was moulded to fill the gap in order to improve contact to the holder (Figure 1b). Microplates were cut into quarters with a hot wire cutter before plasma treatment, so they could be mounted on the sample holder in our small prototype plasma reactor and were taped back together for DNA and streptavidin immobilisation and fluorescence detection.

PIII treatment

PIII treatment was performed using inductively coupled radio frequency (RF) power at 13.56 MHz (ENI radio frequency power generator) to generate plasma and a negative voltage bias applied to the stainless-steel sample holder to accelerate positive ions towards the sample.[38] The pressure inside the chamber was evacuated to less than 5×10^{-5} Torr and high purity nitrogen gas was introduced and maintained at 2 mTorr during the treatment. The RF forwarded power was 100 W with a reverse power of 12 W when matched. Microplates, with or without aluminium foil, were taped on the stainless-steel holder with stainless steel mesh placed 5 cm from the holder and electronically connected to it. Nitrogen ions were accelerated through the mesh towards the stainless-steel holder

with 20 kV negative bias pulses of 20 μs duration at a frequency of 50 Hz. The microplates were treated for 400 or 800 seconds (PIII 400 or PIII 800).

PAC treatment

PAC treatment was performed in a separate plasma system using capacitively coupled RF power at 13.56 MHz (Eni OEM-6) and a negative pulsed bias generated by RUP6 pulse generator (GBS Elektronik GmbH, Dresden, Germany).[39] Microplates with aluminium foil were positioned on a stainless-steel sample holder connected to RUP6 and the chamber was evacuated to less than 5 x 10^{-5} Torr. Prior to the plasma coating, microplates were activated with argon ions to facilitate coating adhesion for 2 minutes at RF power of 75 W and an applied bias of 500 V. The pressure of argon inside the chamber was maintained around 70-80 mTorr. For PAC deposition a reactive gas mixture of acetylene, nitrogen and argon was introduced into the chamber. The ratios between gases were controlled by setting flow rates on mass flow controller (Allicat Scientific) and the pressure inside the chamber during the coating deposition was maintained at 110 mTorr. Plasma deposition was conducted with a plasma discharge of 50 W and a negative bias voltage of 500 V for 10 minutes. Negative bias from RUP 6 was applied with a frequency of 3 kHz and pulse width of 20 μs. Four different gas ratios were chosen for comparison: no nitrogen, low nitrogen, moderate nitrogen, and high nitrogen (Table 1). Separate PAC treatments were performed on smooth silicon wafers with a native oxide layer to measure the coating thickness.

Upon exposure to air, radicals on the treated surfaces react with oxygen in the air to form oxygen containing groups. These changes to the surface chemistry have been previously shown to saturate after a week.[40] Therefore, after each treatment, the microplates were covered in aluminium foil and stored for at least a week in air at room temperature before all subsequent analysis and biomolecule immobilisation.

Treatment	Gas flow rate (SCCM)			% nitrogen
	Acetylene	Nitrogen	Argon	
No nitrogen	1	0	13	0
Low nitrogen	1	3	10	21
Mod nitrogen	1	10	3	71
High nitrogen	1	13	0	93

Table 2: PAC treatments with four different gas flow rate recipes.

Ellipsometry

Ellipsometric spectroscopy was used to calculate the coating thickness of PAC deposited on silicon wafers. Ellipsometric data were collected at three angles of incidence (65°, 70°, and 75°) using a J.A Woollam M2000 V spectroscopic ellipsometer. A model consisting of a silicon substrate, silicon oxide layer (2 nm), and a Cauchy layer to represent the PAC layer was used to fit the data in visible range to obtain the film thickness.

Water contact angle measurements

The substrates were prepared by cutting out the bottom of the wells out from the microplates and placing the surface under a mould which is a 96-well microplate without the well bottoms for PIII and PAC treatment. The surface free energies of PIII and PAC treated TC treated 96 well microplates (1 week post treatment) were calculated and compared to untreated polystyrene. Contact angle measurements using two liquid probes (water and diiodomethane) were performed using a Theta Tensiometer (Biolin Scientific).

Results are averaged over 10 drops for each sample. Surface free energies were calculated using Owens–Wendt-Rabel-Kaelble method.

X-ray photoelectron spectroscopy

The composition of elements present on PIII and PAC treated TC treated 96 well plates were determined by X-ray photoelectron spectroscopy (XPS, Thermo Fisher Scienitific K-Alpha+) with a monochromated Al Kα X-ray source. Ten survey scans and five high resolution scans of major elements (carbon, oxygen, nitrogen and silicon) were taken on each sample for comparison. Element peak areas were divided by element specific sensitivity factors and converted to atomic percentage for each element.

Electron paramagnetic resonance spectroscopy

In order to measure radical densities, polystyrene film (Goodfellow, thickness 0.19 mm) was cut into 40 mm x 5 mm strips and treated with either PIII or PAC. Polystyrene film was used as a proxy for the microplate, which did not fit in the measurement instrument. The microwave absorption by unpaired electrons from the samples were measured using an electron paramagnetic resonance (EPR) spectrometer (Bruker EMX X-band). Measurements were done at room temperature with a microwave power of 2 mW and a frequency of 9.8 MHz. A magnetic field was scanned with a central value of 3523 G and a sweep width of 200 G. Ten scans were measured on each sample. Similar measurement was applied to 2,2diphenyl-1-picrylhydrazyl (DPPH) powder containing EPR tube with known radical density to calculate the number of unpaired electrons on each sample.

Fourier transform infrared attenuated total reflectance (FTIR-ATR) spectroscopy

Changes in surface chemistry after plasma treatment were determined by comparison of FTIR-ATR spectra of untreated and treated polystyrene prior to biomolecule immobilisation. Polystyrene films were cut into small discs and placed at the bottom of microplate wells for PIII and PAC treatment. A week after the treatment, the discs were analysed using a Hyperion FTIR spectrometer (Bruker) equipped with a micro germanium crystal ATR accessory. Each analysis consists of 128 scans with a resolution of 4 cm^{-1}. The spectra were normalised with the intensity of the 1490 cm^{-1} peak of polystyrene for comparison.

Absorbance and autofluorescence measurements

Changes in absorbance and autofluorescence after PIII and PAC treated microplates were measured with PHERAstar FSX (BMG Labtech) and compared to untreated microplates. Absorbance was measured with top optic at 450 nm with 22 flashes per well. Fluorescence intensity was measured at five commonly used excitation and emission wavelengths with five optic modules (460/510, 485/520, 540/580, 575/620, 635-20/680-20). For each end point measurement, the top optic was used to scan the centre of the well with 10 flashes, focal height was adjusted for each sample and the gain was set at 1400.

Immobilisation of single-stranded DNA

The method for immobilisation of single-stranded DNA (ssDNA) was based on previous work with PIII treated polypropylene.[30] A twenty-one nucleotide (nt) ssDNA sequence (IDT DNA) was designed with a linker of 20 additional adenine nucleotides (Table 3). The 20-

A linker had previously been shown to improve DNA attachment to plasma treated surfaces with the correct orientation for DNA hybridisation. It was expected that in acidic conditions the amine groups in the adenine nucleotides of the linker will be protonated, and the linker will therefore be preferentially electrostatically attracted to the negatively charged plasma surface as compared to the core DNA sequence.

Wells of untreated, PIII and PAC treated 96-well microplates were incubated with 40 μL of 2 μM ssDNA in 10 mM of citric acid/sodium citrate buffer at pH 3, 4, 5 or 6 or disodium hydrogen phosphate/sodium dihydrogen phosphate buffer at pH 7 or 8 for one hour at room temperature on a shaker. DNA solution was replaced with 200 μL of 1% BSA in 10 mM PBS at pH 7.4 for one hour at room temperature on a shaker to block the remaining active surface. BSA solution was removed and the wells were washed with 200 μL of 2% SDS three times with vigorous shaking. After rinsing with 200 μL of MilliQ water three times, DNA hybridisation was performed by adding a 21-nt complementary DNA strand with 3' Alexa647 fluorophore modification (IDT DNA, Table 3). Complementary DNA was added to a hybridisation buffer (consisting of 2 mM magnesium chloride (Sigma-Aldrich), 1 x Tris EDTA (Sigma-Aldrich), 1% BSA and 0.6% SDS) to a final concentration of 0.8 μM. Each well was incubated with 40 μL of 0.8 μM complementary DNA solution for one hour on a shaker at room temperature. The same hybridisation process was repeated in a separate well for non-complementary DNA strand with 3' Cy3 fluorophore (Table 3). After removing the solution, the wells were washed with 200 μL 10 mM PBS three times with vigorous shaking. Then, the wells were washed three times with vigorous shaking with 200 μL of each of 3 washing buffers; washing buffer 1 (2 x saline-sodium citrate (SSC) + 0.6% SDS), washing buffer 2 (0.2 x SSC + 0.6%SDS), and washing buffer 3 (0.1 x SSC + 0.5% Tween 20). After rinsing the wells with 200 μL of 10 mM PBS, each well was filled with 40 μL of 10 mM PBS for fluorescence intensity measurement.

The fluorescence intensity of the Alexa647 and Cy3 modification on the complementary and non-complementary DNA was measured with 635-20/680-20 and 540/580 optic modules on PHERAstar FSX, respectively. For each measurement, the top optic was used to scan a 10 x 10 matrix of well diameter 3-5 mm with 10 flashes at each scan point. Focal height was adjusted for each sample and the gain was set at 2000.

Immobilisation of streptavidin and attachment of biotin-DNA

Wells of plasma treated and untreated microplates were incubated with 40 μL of 10 μg/mL streptavidin-Cy3 (Sigma-Aldrich, P6402) in 10 mM of citric acid/sodium citrate buffer at pH 3, 4, 5 or 6 or disodium hydrogen phosphate/sodium dihydrogen phosphate buffer at pH 7 or 8 for one hour at room temperature on a shaker. Streptavidin solution was replaced with 200 μL of 1% BSA in 10 mM PBS at pH 7.4 for one hour at room temperature on a shaker to block the remaining active surface. BSA solution was removed and the wells were rinsed with 200 μL of 10 mM PBS three times. After rinsing, each well was washed with 200 μL of 10% Triton in 10 mM PBS three times. Next the wells were rinsed with 200 μL of 10 mM PBS for three times, then the wells were incubated with 2 μM 5' biotin-modified ssDNA (IDT DNA, Table 3) in 10 mM PBS at pH 7.4 for one hour at room temperature on a shaker. Following biotin-DNA incubation, the wells were incubated with the Alexa647-modified complementary DNA, as described in the DNA immobilisation method. The hybridised surface was washed with 200 μL of washing buffer 4 (2 x SSC + 0.05% Tween 20) three times before rinsing with 10 mM PBS. PHERAstar FSX fluorescence plate reader with optic modules 540/580 and 635-20/680-20 was used to detect immobilised streptavidin-Cy3 and the hybridised complementary Alexa647-DNA, respectively. For each measurement, the top optic was used to scan 10 x 10 matrix of well diameter 3-5 mm with 10 flashes at each scan point. Focal height was adjusted for each sample and the gain was set at 1000.

Table 3: Sequences of immobilising DNA, hybridising DNA and biotin DNA to bind to immobilised streptavidin

DNA name	DNA sequence
immobilising DNA	20xA-GCTCTGCAATCAACTTATCCC
hybridising DNA	GGGATAAGTTGATTGCAGAGC-Alexa647
wrong hybridising DNA	GTGATGTAGGTGGTAGAGGAA-Cy3
biotin DNA	biotin-GCTCTGCAATCAACTTATCCC

Results and discussion

The amount of DNA or protein that can be usefully immobilised on a PIII or PAC microplate depends on the surface chemistry, optical properties, immobilisation density, and orientation of biomolecules on the treated surface. PIII treatment introduces long-lived radicals into a modified surface layer,[41,42] while PAC treatment deposits a polymer coating with a high concentration of long-lived radicals on surfaces.[43–45] PIII treatment leads to changes in nitrogen content,[26,38,41] while PAC results in deposition of a layer of hydrogenated amorphous carbon nitride from a mixture of acetylene and nitrogen gases,[45] and both surfaces undergo oxidation on exposure to air after treatment leading to changes in oxygen content. Wettability, surface energy, optical absorbance and autofluorescence are also known to be affected by PIII and PAC treatments.[26,29] To determine the optimal PIII and PAC treatment recipes for DNA and streptavidin immobilised microplates, the chemical properties of treated microplates were studied and then compared, including elemental composition, radical density, wettability and surface energy. Optical absorbance and autofluoresence were similarly characterised and compared. Following this, the optimal treatment conditions were determined for high density DNA and streptavidin immobilisation on microplates. The hybridisation efficiency of DNA-modified microplates and biotin binding efficiency of Streptavidin-modified

microplates were determined to evaluate the useful binding capacity of the treated microplates.

Chemical Properties of PIII treated microplates

The chemical composition of PIII treated microplates was determined by XPS, comparing 400 s (PIII-400) and 800 s (PIII-800) treatment times (Figure 2a). The oxygen content of the PIII treated microplates (6.1-11.1%) was not significantly different to the TC-treated microplate (8.3%). Similarly, surface nitrogen content was very low both before (0.6%) and after PIII treatment (0.5-0.8%). This was surprising, as previous studies have shown an increase in nitrogen content (7-12%) following 400 s PIII treatment of glass coverslips spin-coated with polystyrene,[26] and an increase in oxygen composition from exposure to air following treatment of polystyrene film.[40] Differences in the results observed here may be due to the deep well shape or differences in the type of polystyrene structure, such as the orientation of phenol groups, of the microplates as compared to polystyrene film or spin-coated layers. The deconvolution of C 1s peaks are shown in the supporting information (Supporting Figure S1). FTIR-ATR spectra did not show a noticeable difference between PIII-400 and PIII-800 (Supporting Figure S2).

Long-lived radicals appearing in the modified surface layer have been proposed as the main mechanism underlying covalent immobilisation of biomolecules on PIII surfaces.[32] Radical densities of radicals in the samples can be calculated from EPR intensities by comparing with that obtained from a standard 2,2-diphenyl-1-picrylhydrazyl (DPPH) sample with known radical density. However, due to the difference in geometry and volume (DPPH powder was put in an EPR tube while PIII and PAC treated PS strips were mounted on an EPR tube), we could not calculate the exact radical density on our samples. Instead, we compared the relative density of radicals in those samples by normalising with the depth of the plasma treatment with the assumption that the measurement areas are the same for all samples.

For PIII samples, the depth of treatment was assumed as 75 nm from the literature.[38]

The relative density of radicals on treated microplates was found here to increase significantly (one-way ANOVA, $p < 0.0001$) after both 400 s and 800 s PIII treatments (0.10 ± 0.001 and 0.24 ± 0.0003 respectively) compared to UT PS microplates (1.12×10^{-6}, Figure 2b, Supporting Figure S3). The increase from PIII-400 to PIII-800 was also significant (one-way ANOVA, $p < 0.0001$). These results agree with previous studies which have shown an increase in long-lived radical density with increasing PIII treatment time, which has been suggested to be due to an increased concentration of both dangling bonds and carbonised clusters that serve to stabilise the unpaired electrons in the radicals.[42]

Wettability of surfaces is another property known to be affected by PIII treatment. Here, PIII treatment was observed to significantly (one-way ANOVA, $p < 0.0001$) decrease the water contact angle of PIII-400 (45.5 ± 1.7°) and PIII-800 (37.0 ± 1.9°) treated microplates, compared to TC-treated microplates (79.1 ± 0.6°) (Figure 2d). In contrast, previous studies found that water contact angles of PIII treated flat substrates increased with treatment time.[26,40] The shape of the microplates may have contributed to this difference in trend. The Owens–Wendt-Rabel-Kaelble method considers the surface energy to be comprised of a polar component and a dispersive component. Polar components of PIII treated microplates (23.7 ± 0.3 - 30.1 ± 0.3 mJ/m^2) were found to be significantly higher than TC-treated microplates (4.8 ± 0.1 mJ/m^2, one-way ANOVA, $p < 0.0001$), and increased with treatment time (Figure 2e). The wettability and polar surface energy component values for the PIII treated microplates had a stronger correlation to the relative density of radicals as described above, than to the surface nitrogen and oxygen composition, which agrees with previous findings.[46]
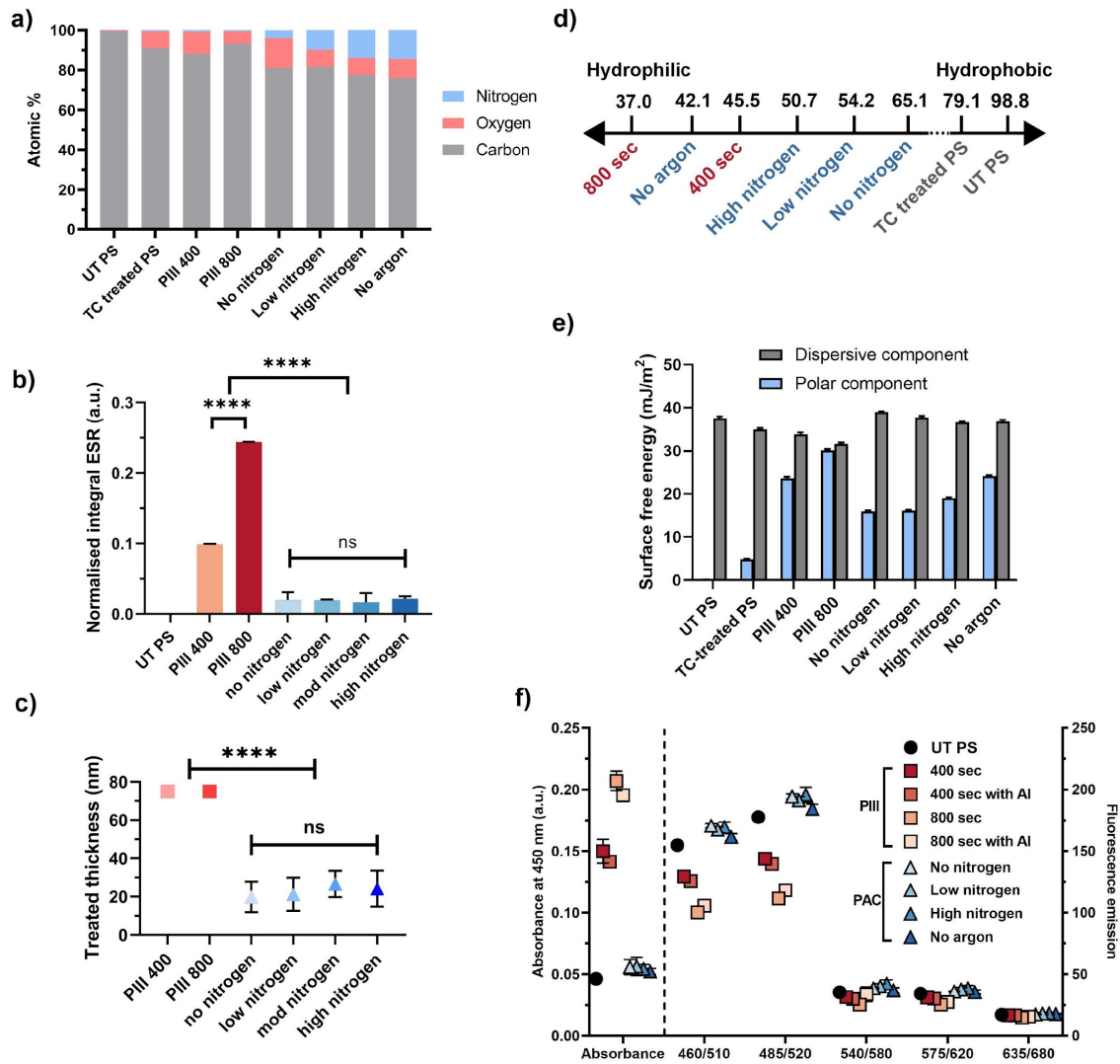
Figure 2: (a) Percentage surface elemental concentration of UT, TC, PIII and PAC treated PS microplates. (b) Comparison of relative electron paramagnetic resonance (EPR) integral intensity between UT PS, PIII and PAC treated PS. Measured EPR signal was integrated and normalised by the depth of radical penetration (PIII) or thickness of deposition layers (PAC). (c) Effective depth of the PIII treatment on polystyrene[38] and PAC thickness obtained from ellipsometry measurement of PAC treated silicon wafers. (d) Water contact angles of UT, TC, PIII and PAC treated PS sheets placed in 96 well microplates during plasma treatment. (e) Dispersive and polar components of surface free energy of UT, TC, PIII and PAC treated PS microplates, calculated from the Owens–Wendt-Rabel-Kaelble method. The error bars represent their standard errors. (f) Mean absorbance and autofluorescence with SD of UT (circles), PIII (squares) and PAC (triangles) treated PS microplates. SD bars are hidden when they are smaller than the marker size. The left column and y-axis show absorbance at 450 nm and the right column and y-axis show the autofluorescence emission intensity at five excitation/emission wavelengths.

Chemical Properties of PAC treated microplates

The chemical composition of PAC microplates was determined by XPS, comparing four different gas recipes containing increasing amounts of nitrogen; no nitrogen, low nitrogen, moderate (mod) nitrogen and high nitrogen (Figure 2a, Supporting Figure S1). Surface nitrogen was found to increase with nitrogen content in the gas mixture across all PAC recipes. Values measured were TC (0.6%), to no nitrogen (4.0%), low nitrogen (9.7%), mod nitrogen (13.8%), and high nitrogen PAC (14.6%). For surface oxygen, no nitrogen PAC treated microplates had increased surface oxygen (14.9%). All other recipes had oxygen content (8.5 - 9.4%) similar to that of TC-treated microplates (8.3%). It is important to note that the sampling depth measured by XPS (about 10 nm) may include the polystyrene substrate below the deposited layer, which would lower the nitrogen percentage. The nitrogen trend observed here agrees with observations made previously.[29] Other work has shown that deposited coatings can have as much as 35% nitrogen and 12.5% oxygen,[44] however the use of a different substrate (stainless steel) prevents quantitative comparison of the results because the stainless steel composition can be removed from the calculation of atomic composition. FTIR-ATR spectra did not show a significant difference between the four PAC recipes (Supporting Figure S2).

There was no significant difference between the relative density of radicals in different PAC treated samples (Figure 2b, no nitrogen 0.020 ± 0.01, low nitrogen 0.019 ± 0.0008 , mod nitrogen 0.016 ± 0.013, high nitrogen 0.021 ± 0.0035). As described above, these values were normalised with the PAC coating thickness (Figure 2c). The water contact angles of the microplates decreased after PAC treatment (Figure 2d). There was no significant difference in water contact angles between low and mod nitrogen PAC, but the hydrophilicity of high nitrogen was significantly higher than that of no nitrogen (one-way ANOVA, $p<0.0001$). The water contact angles ranged between 42.1°and 65.1°. This trend

is similar to previous findings with PAC treated stainless steel.[29] The polar component of PAC samples also increased with increasing amount of nitrogen in the PAC recipe.

Comparison of Chemical Properties of PIII and PAC modified microplates

Overall, PIII microplates were found to have low surface nitrogen composition, high relative density of radicals and were very hydrophilic. PAC microplates had high nitrogen composition, moderate relative density of radicals and were more hydrophilic than untreated plates. PIII and PAC treated microplates were found to differ in several measured parameters. PAC treated microplates had significantly higher amounts of surface nitrogen compared to PIII treated microplates (PIII 0.5-0.8%, PAC 4-14.6%), while PIII treated microplates had higher relative density of radicals (PIII 0.10-0.24, PAC 0.016-0.021) and were more hydrophilic (37.0°-45.5°) compared to all PAC (50.7°-65.1°) except the high nitrogen condition (42.1°). The relative density of radicals appeared to have a greater correlation with surface hydrophilicity than surface nitrogen and oxygen compositions.

Comparison of Optical Properties of PIII and PAC modified microplates

Changes in optical properties can impact the utility of plasma activated microplates, because optical readout is the main method of detection for biochemical plate assays. Thus, the effects of PIII and PAC treatment on absorbance and autofluorescence were characterised (Figure 2f). Absorbance was measured at 450 nm as this wavelength is used in many assays such as HRP colorimetric assay.[27] The absorption spectra of PIII and PAC treated microplates are shown in Supporting Figure S4. Mean absorbance at 450 nm was found to be significantly higher (one-way ANOVA, $p<0.0001$) for PIII (0.150-0.207 a.u.) and PAC (0.052-0.056 a.u.) compared to untreated microplates (0.046 ± 0.001 a.u.). The greatest increase in the absorbance was observed for PIII-800 (0.207 ± 0.008

a.u.), followed by PIII-400 (0.150 ± 0.010 a.u.). Browning of the clear microplates by PIII treatment is in good agreement with previous observation was explained from the forming of carbonised structures in the modified layer, which increase in number and size with longer treatment times.[26,47] PIII samples with aluminium had smaller variance in absorbance over multiple wells (0.016 a.u.) compared to the non-aluminium samples (0.030 a.u.), suggesting that the aluminium modification improved the uniformity of treatment across the microplate. PAC treated microplates had much smaller increase in absorbance (1.13-1.22 fold) compared to PIII treated microplates (3.36-4.5 fold), with no significant difference between PAC gas recipes (0.052-0.056 a.u., oneway ANOVA, p>0.1). It is known that PIII treatment causes deeper surface changes (75 nm) compared to PAC (19.9-26.6 nm),[38] which may lead to the greater increase in optical absorbance observed here. Absorbance normalised by the treatment depth is shown in Supporting Information (Supporting Figure S5). Overall, PIII resulted in a large (288%) increase in absorbance at 450 nm relative to untreated microplate, while PAC had a more modest (17.5%) relative increase.

Generally, aromatic polymers have high autofluorescence at shorter wavelength due to low energy π to π^* transitions.[48] This agrees with observations here, with all untreated and treated microplates having higher autofluorescence at shorter wavelengths (460/510 and 485/520 nm) than at longer wavelengths (540/580, 575/620, 635/680 nm). In addition to this trend, PAC treated microplates also had significantly higher autofluorescence at shorter wavelengths (162-196, one-way ANOVA, p<0.0001) compared to untreated (155-157), while PIII treated had significantly lower (100-144, one-way ANOVA, p<0.0001). Plasma treatment leads to the formation of highly conjugated double bond structures and aromatic rings,[40] which may explain the increase in autofluorescence observed for PAC samples. In PIII treatment, heavy ion bombardment induces amorphous carbon structure on polymer surface which explains the lower autofluorescence observed for PIII and supported by the observation that PIII-800 had lower autofluorescence (100-118) than

PIII-400 (126-144). In contrast, at longer wavelengths, there is less difference in autofluorescene across all samples. Previously, PIII-800 treated PS coated glass had been observed to have higher autofluorescence at longer excitation wavelength (631 nm) compared to a shorter (488 nm).[26] However, optical measurements are a combination of surface and substrate properties, so differences to results here are likely due to substrate differences. Thus, overall PAC and PIII treatments changed microplate autofluorescence at shorter wavelengths (510 - 520 nm), but they had smaller changes at longer wavelengths (580 - 680 nm). The changes at shorter wavelengths were small relative to total autofluorescence from the polystyrene substrate, with PAC giving an 8% increase and PIII a 27% decrease. At longer wavelengths, PAC had a 9% increase and PIII had a 14% decrease from untreated polystyrene.

DNA Oligonucleotide immobilisation

For applications in DNA-binding assays it is important for the immobilised DNA to maintain its ability to hybridise with complementary DNA. Therefore, measurements focused on the density of hybridised DNA, as detected by an Alexa-647 fluorophore covalently attached to the hybridising DNA oligonucleotide. Relative immobilised DNA density is shown in Supporting Figure S8. To correctly detect only DNA hybridised to covalently immobilised DNA, wash steps are required to remove non-specifically bound DNA.[10] Wash steps were included to remove non-covalently bound ssDNA (step 4, Figure 3a) and nonhybridised ssDNA from the microplates (step 7-11, Figure 3a). Wash methods selected were based on previous work,[24,28,30] and were found to be effective at reducing the fluorescence signal of negative controls back to the baseline level (t-test, $p < 0.0001$), for both controls with no immobilising ssDNA (step 2) or addition of the wrong sequence of hybridising DNA (step 6, Figure 3c). For example, giving a 50% decrease from step 7 to 11, which is equivalent to approximately 8.4×10^{10} DNA molecules removed from the surface. In preliminary measurements, the density of hybridised DNA was found to be

higher in the centre of the microplate wells compared to the edges (Figure 3b and Supporting Figure S6). Well edges are known to have less efficient fluid mixing[49] and experience lower flux of implanting ions due to shadowing and the reduction of sheath area to wall area ratio, which would limit DNA density near the edge. Therefore, measurements of hybridisation density were averaged over a circle of 3 mm diameter at the centre of the wells, which had a total diameter of 5 mm.

We further quantified DNA distribution homogeneity by comparing an average over a circle of varying diameter at centre of the well to the total well area. DNA density was found to be higher at the well centre, with a trend of decreasing density away from the well centre to the edges across all recipes (Figure 3b and 3c). However, the % change in density was found to be different between the four PAC recipes. DNA is hybridised more homogeneously across the well in moderate and high nitrogen PAC treated wells (average signal across the well reduced by 22.5% on increase in area sampled). Therefore, these recipes would be suitable when more uniform and less crowded DNA immobilised surfaces are required. Low nitrogen PAC treated wells had overall higher DNA density compared to those of moderate and high nitrogen, and better homogeneity of hybridised DNA compared to no nitrogen PAC but less than moderate or high nitrogen PAC (average signal across the well reduced by 31.5% on increase in area sampled). When high density DNA immobilised surfaces are required, low nitrogen PAC treated plates would be the best choice..
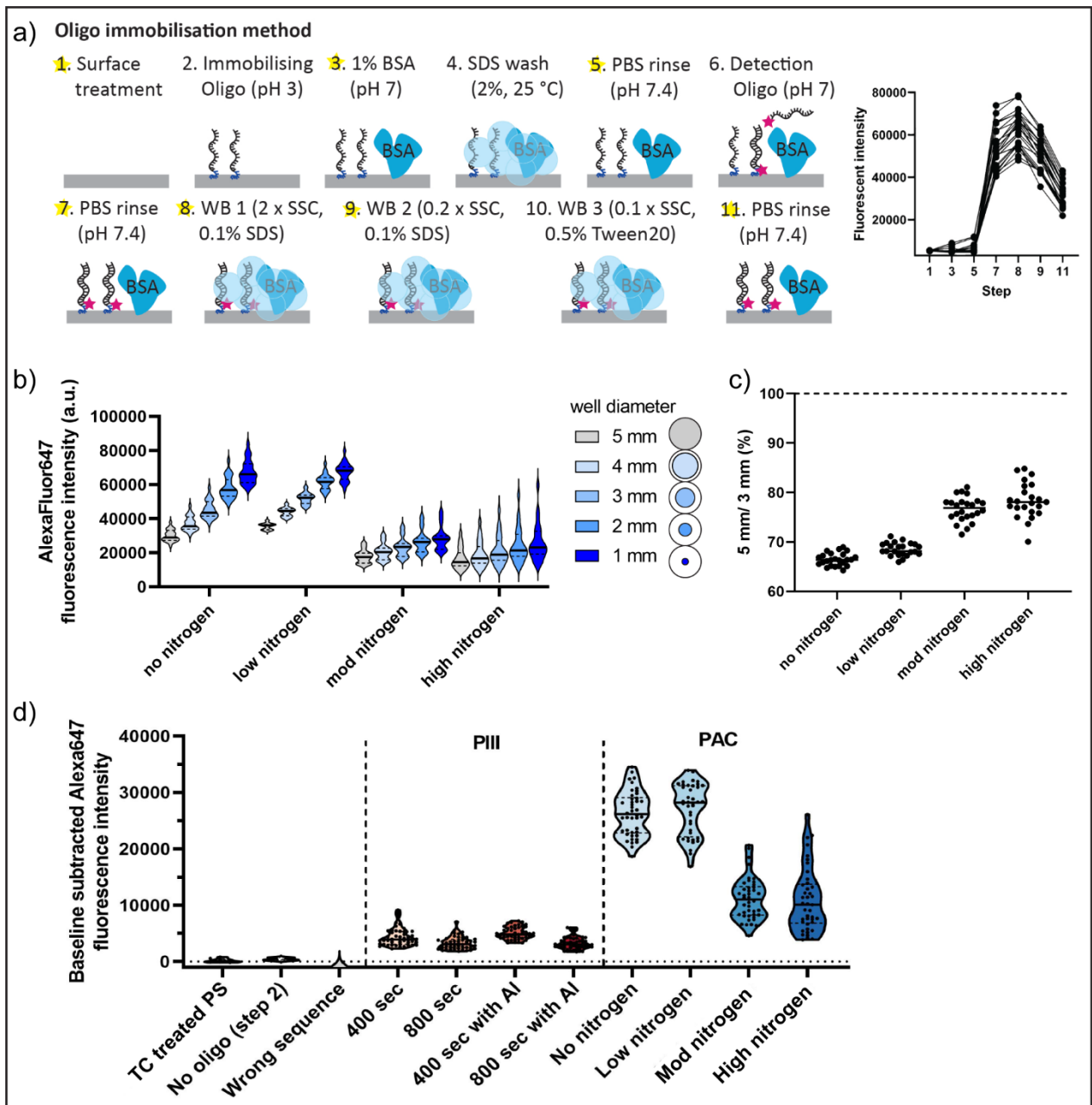
Figure 3: (a) Schematic diagram showing oligonucleotide immobilisation methods and an example of data plotted on the graph on the right-hand side. Fluorescence intensity was measured at yellow highlighted steps and shown on the graph. (b) Hybridised DNA distribution within the well on PAC treated microplates. Fluorescence intensities were measured with well scan mode at diameter 1-5 mm within each well and the average of each diameter is plotted in the graph. (c) Ratio of well average fluorescence intensity at 5 mm to the one at 3 mm. Dotted line at 100% represents a completely homogenous density of DNA across the well area. (d) Baseline subtracted Alexa647 fluorescence intensity of DNA immobilised (pH 4) and hybridised on TC, PIII and PAC treated microplates. The

fluorescence spectra of DNA immobilised low nitrogen PAC is shown in Supporting Figure S7.
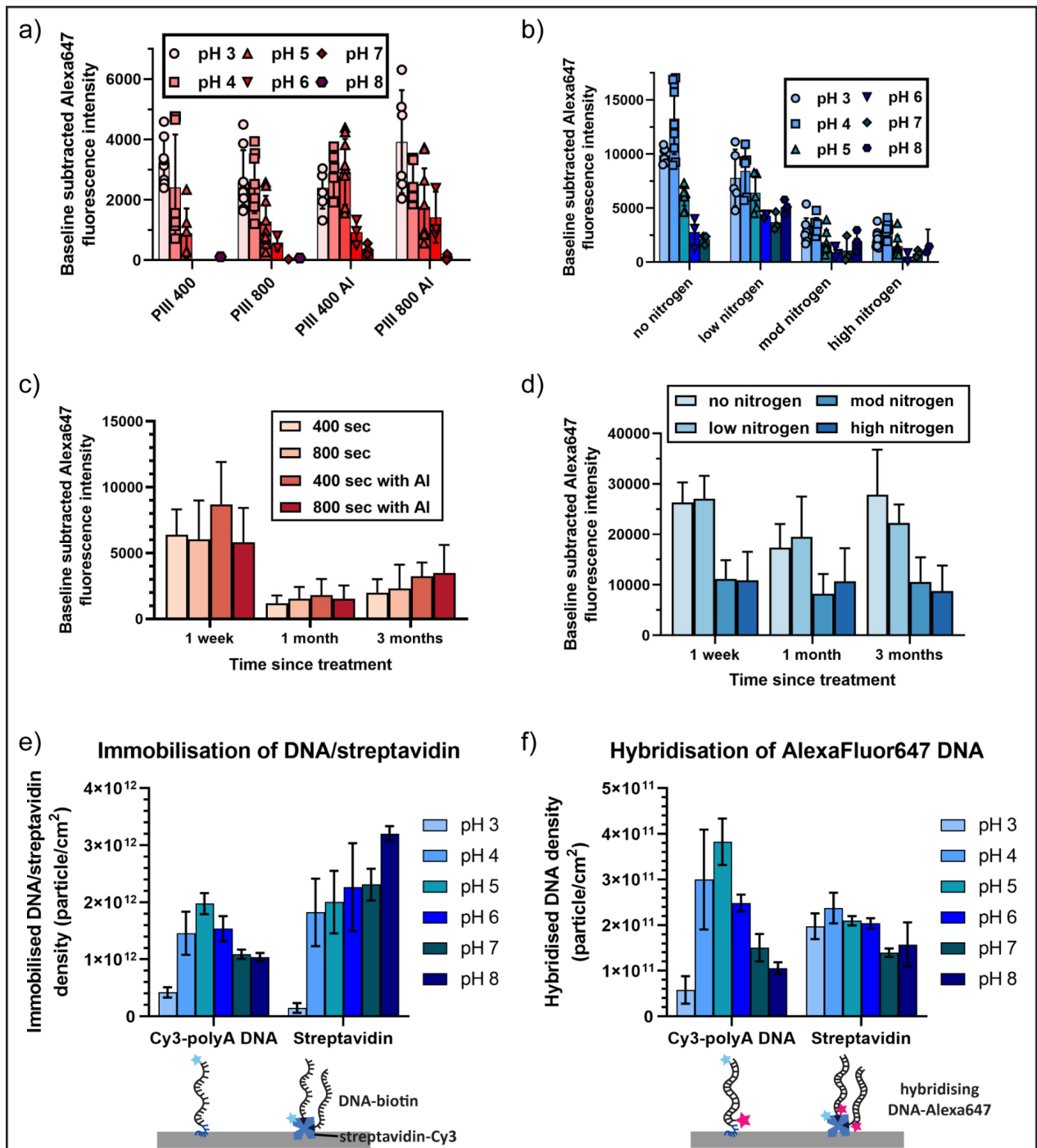

Figure 4: (a) DNA immobilisation and hybridisation on PIII treated microplates at pH 3-8. (b) DNA immobilisation and hybridisation on PAC treated microplates at pH 3-8. (c) DNA

immobilisation and hybridisation to PIII treated microplates 1 week, 1 month and 3 months after treatment. (d) DNA immobilisation and hybridisation to PAC treated microplates 1 week, 1 month and 3 months after the treatment. PAC treated plates were stored at room temperature for 1 week, 1 month or 3 months before DNA immobilisation and hybridisation. (e) Immobilised DNA and streptavidin density on low nitrogen PAC treated 384-well microplate at pH 3-8. (f) Hybridised AlexaFluor647 DNA density on DNA and streptavidin immobilised low nitrogen PAC treated 384-well microplate (pH refers to immobilisation pH).

DNA hybridisation was characterised for all recipes of PIII (PIII-400, PIII-800) and PAC (no, low, mod and high nitrogen). Greater fluorescence signal, indicating higher DNA hybridisation density, was observed for all plasma treated samples compared to the negative controls (<3.1 x 10^{10} molecules/cm^2), and was also higher on PAC than PIII treated microplates (PIII 1.3 x 10^{11} molecules/cm^2, PAC 3.4 x 10^{11} molecules/cm^2, one-way ANOVA, $p<0.0001$) (Figure 3c, Table 4). There was no hybridisation when wrong sequence (non-complementary) DNA was used which indicates that the DNA is only binding through specific base-pairing. DNA hybridisation was approximately 2-5 fold denser on PAC compared to PIII (1.1-1.6 x 10^{11} molecules/cm^2, one-way ANOVA, $p<0.0001$), and no nitrogen and low nitrogen PAC recipes had the greatest amount of hybridised DNA overall (4.7-4.8 x 10^{11} molecules/cm^2, one-way ANOVA, $p<0.0001$). There was no significant difference between the four different PIII surfaces, indicating that the aluminium foil and the treatment time did not affect DNA immobilisation. The effect of pH on DNA immobilisation was tested by incubating immobilising ssDNA in pH 3 to 8 (step 2, Figure 3a). The highest hybridisation density was observed for pH 3 and 4 for almost all PIII and PAC treated microplates (Figure 4a, b). The stability of plasma treated plates over time before DNA immobilisation and hybridisation was also investigated. DNA immobilisation capability of PIII treated microplates decreased one month after the PIII treatment, but there was no further reduction up to three months (Figure 4c). All PAC

samples retained the same DNA immobilisation capability up to three months (Figure 4d).

DNA immobilisation and hybridisation on no and low nitrogen PAC samples were further

optimised by using freshly prepared hybridisation solution and measuring fluorescence

intensity from 3 mm diameter instead of 5 mm diameter. After further optimisation, the

average hybridised density on no and low nitrogen increased to 5.2 x 10^{12} molecules/cm^2

(Supporting Figure S9).

Low nitrogen PAC treatment was also applied to 384-well microplates (PerkinElmer,

OptiPlate-384 black) for immobilisation of DNA and streptavidin (Figure 4e). DNA and

streptavidin immobilised at high densities on the low nitrogen PAC treated 384-well

microplates (2 x 10^{12} and 3.2 x 10^{12} molecules/cm^2 respectively). The hybridisation

densities of AlexaFluor647 DNA on the 384-well microplates were similar to the results

from 96-well microplates (Figure 4f, 2.4 - 3.8 x 10^{11} molecules/cm^2).

Surface modification	Hybridisation density (x 10^{11} molecules/cm^2)	SA density (x 10^{11} molecules/cm^2
TC treated	0.3	0.01
PIII-400	1.2	0.64
PIII-800	1.1	0.61
PIII-400 with Al	1.6	0.84
PIII-800 with Al	1.1	0.79
No nitrogen	4.8	2.2
Low nitrogen	4.7	9.0

Mod nitrogen	2.0	4.3
High nitrogen	2.0	4.0

Table 4: Hybridised DNA and immobilised streptavidin densities of TC, PIII and PAC microplates

Interestingly, the measured relative density of radicals was found not to correlate with the amount of DNA hybridised to the surface. PIII microplates had 5-15 fold higher relative density of radicals than PAC, but a 2-5 fold lower DNA hybridisation capacity. This demonstrates that the low amount of radicals on PAC surfaces was sufficient for dense DNA immobilisation. Previously, it was reported that electrostatic and hydrophobic forces played important roles in immobilisation of yeast cells on PIII treated surfaces.[50] Similarly, here we found stronger correlations between surface charge and hydrophobicity of treated surfaces and the amount of immobilised and hybridised DNA.

Intermolecular interactions between DNA and the surface are important because the DNA needs to come close to the surface to react with the radicals and form covalent bonds. DNA adsorption to surfaces is impacted by long range electrostatic forces and short range forces such as van der Waals (vdW).[51] Plasma treated surfaces are known to be negatively charged at higher pH and more neutrally charged at lower pH.[50] At neutral pH, each phosphate group on the DNA backbone has a negative charge with a pK_a <2, and all bases are neutrally charged.[52] Therefore, it is expected that there will be an electrostatic repulsion between the surface and DNA at neutral pH which scales with $1/r^2$, where r is the distance between the two species.[51,53] By using lower pH during immobilisation, DNA density improved significantly. At lower pH, it is expected that surface nitrogen and oxygen groups are protonated and become less negatively charged.[50] Similarly, nucleobases adenine and cytosine are also expected to be protonated (pK_a 3.52, 4.17 respectively),[52] and thus the polyadenine spacer on the immobilising DNA

strand will become less negatively charged.[50,51] Note that DNA has good stability at pH 3 for at least one hour which is the condition used here for DNA immobilisation, but that depurination can occur at lower pH.[51] PAC surfaces had higher DNA density than PIII, which could be explained by the higher composition of nitrogen that could be protonated on PAC surfaces leading to more favourable electrostatic interactions. However, the highest DNA density was found on PAC surfaces with lower composition of surface nitrogen. Thus, charge interactions cannot fully explain the results observed.

Hydrophilicity of the surface is another important factor that could affect the intermolecular interaction with DNA. Both hydrophilic and hydrophobic surfaces can attract DNA.[53] Hydrophobic surfaces can attract nearby DNA through short range vdW forces, and hydrophilic surfaces can attract longer-range DNA via dipole-dipole and hydrogen bonding. However, hydrophilic surfaces are more susceptible to form a dense hydration layer which competes with intermolecular attraction between the surface and DNA via hydrogen bonding. Thus, higher DNA density on the no nitrogen and low nitrogen PAC surfaces compared to other samples could be explained by their relative hydrophobicity compared to mod and high nitrogen PAC and all PIII conditions, which minimises formation of the hydration layer and maximises vdW forces.

Streptavidin immobilisation

Streptavidin immobilised on plasma treated surfaces was directly detected by the fluorescence of covalently modified Cy3 streptavidin. For PAC surfaces it was also indirectly detected by binding with dual biotin-modified Alexa647-modified DNA strands. While the former quantifies protein immobilised, the latter will only detect active protein on the surface. Similar to DNA, streptavidin was also found to bind more on PAC treated microplates than PIII treated microplates (Figure 5a), with significant increase for all

plasma treated conditions above the non-treated control (TC treated 0.01×10^{11} molecules/cm^2, PIII 0.7×10^{11} molecules/cm^2, PAC 4.9×10^{11} molecules/cm^2, one-way ANOVA, $p<0.0001$). In contrast to DNA, low nitrogen PAC had the highest amount of bound streptavidin (no nitrogen 2.2×10^{11} molecules/cm^2, low nitrogen 9.0×10^{11} molecules/cm^2, mod nitrogen 4.3×10^{11} molecules/cm^2, high nitrogen 4.0×10^{11} molecules/cm^2), whereas DNA immobilisation on both low and no nitrogen PAC were similar. This trend observed on PAC surfaces was reproduced for biotin-DNA binding, indicating that the immobilised protein remains available for biotin binding (Figure 5b, no nitrogen 0.6×10^{11}, low nitrogen 12.2×10^{11}, mod nitrogen 7.3×10^{11}, high nitrogen 7.8×10^{11} biotin-DNA molecules/cm^2). There was no DNA hybridisation to bound biotin-DNA when wrong sequence DNA was used. By calculation, there were an average of 2.14 hybridised DNA-biotin molecules bound to each immobilised streptavidin on the surface. The best PIII surface for streptavidin immobilisation was PIII-400 with aluminium, but it had about 10-fold less streptavidin compared to the best PAC condition. The pH of immobilisation buffers influenced the amount of immobilised streptavidin on PIII and PAC microplates. For PIII microplates, the optimum immobilisation was achieved at pH 5 (Figure 5c). For PAC microplates, optimum streptavidin immobilisation was achieved at pH 5 for no nitrogen PAC, and at pH 4-7 for the other PAC recipes (Figure 5d). The stability of PIII treated microplates deteriorated significantly after one month as reflected by its capability to immobilise streptavidin (Figure 5e). However, the capability to immobilise streptavidin did not change significantly for PAC samples up to 3 months old (Figure 5f).
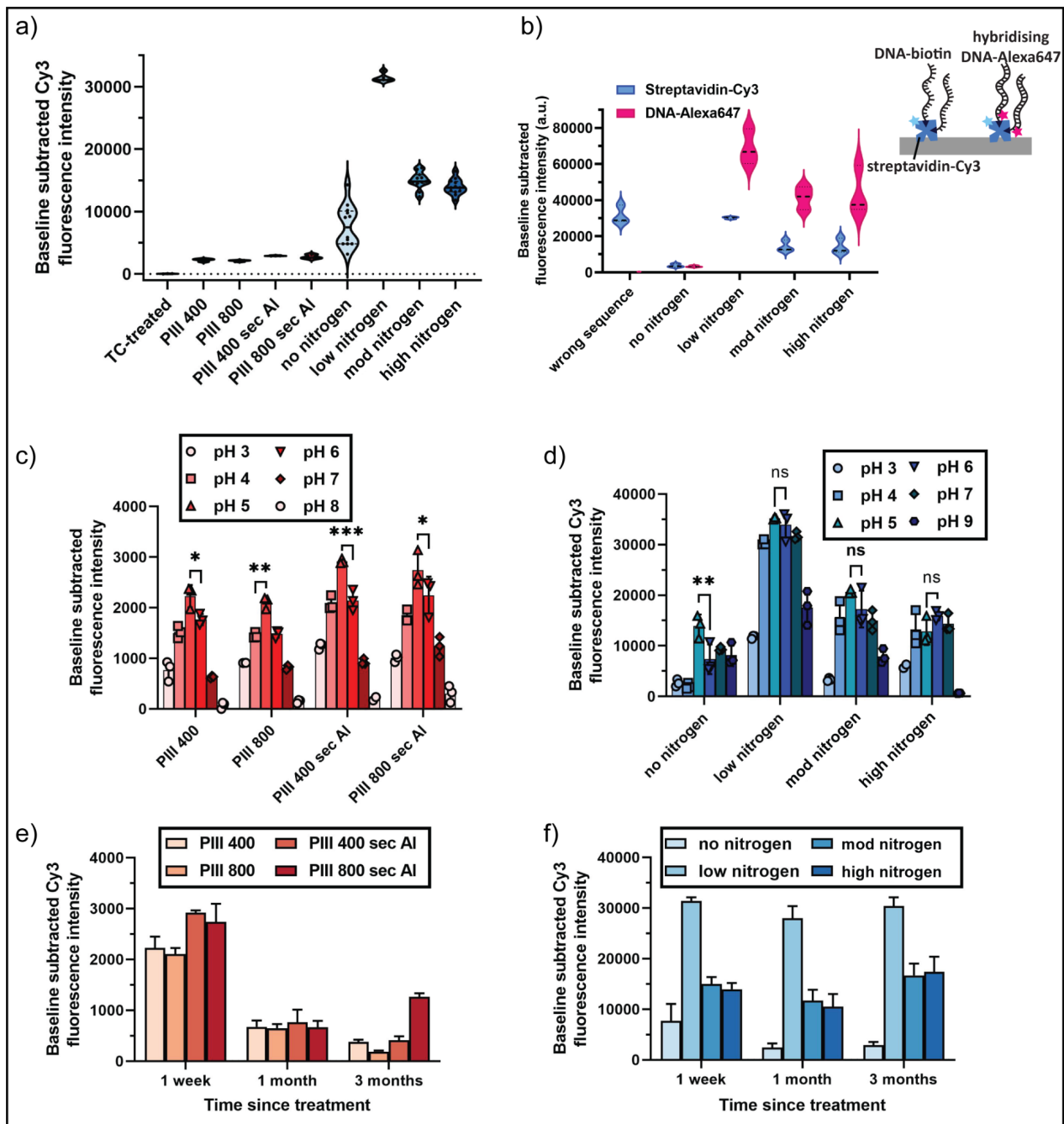
Figure 5: Streptavidin immobilisation to microplates. (a) Cy3 fluorescence intensity of streptavidin-Cy3 immobilised on TC, PIII and PAC treated microplates. (b) Ability of immobilised streptavidin to bind with biotin. (c) Streptavidin immobilisation to PIII treated microplates at pH 3-9. (d) Streptavidin immobilisation to PAC treated microplates at pH 3-9. (e) Streptavidin immobilisation to 1 week, 1 month and 3 months old PIII treated microplates. (f) Streptavidin immobilisation to 1 week, 1 month and 3 months old PAC

treated microplates. Fluorescence spectra of streptavidin immobilised low nitrogen PAC are shown in Supporting Figure S7.

These results suggest that the immobilisation of streptavidin to PIII and PAC surfaces is also dominated by electrostatic interactions and surface hydrophilicity. Streptavidin has pI of 5 which matches with the optimum immobilisation pH found on both PIII and PAC surfaces. This indicates that neutrally charged streptavidin is favourable for immobilisation. Zero charge on the protein may result in better packing of protein on the surface as it eliminates repulsion between protein molecules as they arrive at the surface. This phenomenon is very interesting, and needs further investigation with other proteins to study their optimum immobilisation pH. Streptavidin is very hydrophilic, and it is known to be more attracted to hydrophilic surfaces.[54] However, it did not bind well to PIII treated surfaces even though they were the most hydrophilic surfaces of all. Again, it could be that on very hydrophilic PIII and PAC surfaces there is a dense hydration layer, which limits streptavidin binding on more hydrophilic surfaces. Low nitrogen PAC surfaces may have a good balance between hydrophobicity and hydrophilicity, which minimises competition with water. However, further investigation of the surface properties is required to confirm these proposed mechanisms.

Summary of optimised conditions

PIII and PAC plasma treatment of 96-well polystyrene microplates resulted in covalently immobilised DNA and streptavidin, in a single step without the use of linkers. High density DNA immobilisation was achieved on no and low nitrogen PAC at pH 3-4. Streptavidin immobilisation was optimal on low nitrogen PAC treated microplates at pH 5-7. These PAC treated microplates remained active for the immobilisation for at least three months.

The maximum hybridised DNA density obtained with no and low nitrogen PAC was about 5.2×10^{12} molecules/cm^2, which is similar to the values reported in studies that use chemically activated surfaces to covalently immobilise DNA[55,56] (Table 1). PAC treatment simplifies the microplate functionalisation process and eliminates risks associated with additional reagents. The current process time to modify microplates with plasma treatment takes 15 minutes, which does not include evacuation and venting time. A scaled-up plasma system will allow multiple plates to be treated at a time and therefore, reduce the manufacturing time and cost.

Despite these benefits, the exact mechanism for covalent immobilisation of biomolecules to plasma treated surfaces is still not fully characterised. This makes it difficult to predict the best conditions for new applications with different biomolecules. While surface biomolecule density did not correlate with radical density, it was observed to be affected by surface nitrogen composition, charge interactions and hydrophilicity. For new applications, optimisation of immobilisation conditions, such as pH and PAC gas mixture would still be required. In the future it could be useful to create a library of reference proteins with different pI to help estimate the optimal immobilisation pH. Also, PAC surfaces were found to have slightly higher background fluorescence at lower wavelength (8% increase from UT), which is important to consider for selection of compatible fluorophores for optical detection. Currently, plasma treated microplates remain stable up to 3 months, however the long-term stability of the DNA and streptavidin coated microplates are not known, and requires further characterisation.

Conclusions

PAC surfaces were found to have more nitrogen and lower radical density, were more hydrophobic and more stable over 3 months than PIII surfaces. Optimal conditions were obtained for high density DNA (PAC, 0% or 21% nitrogen, pH 3-4) and streptavidin (PAC, 21% nitrogen, pH 5-7) binding. DNA hybridisation and protein activity of immobilised molecules were confirmed on 96 and 384 well plates. We show that PAC activated microplates allow for high density covalent immobilisation of functional DNA and protein in a single step, without specific linker chemistry.

PAC biomolecule immobilised microplates could be used for a range of new applications. For example, DNA based assays such as solid phase PCR to capture complementary DNA from clinical samples for PCR reactions. The sequence of the DNA can be altered as long as it has a 20-adenine tail. Streptavidin immobilised microplates could be used to tether any molecules with biotin modifications. Additionally, other biomolecules could be immobilised on PAC treated microplates without using any additional linkers. For example, PAC treated microplates could be coated with avidin or antibody binding proteins, then colorimetric or fluorescence assays could be performed for the detection of biomolecules. Alternatively, PAC treated microplates could be used as a cell culture platform by attaching extracellular matrix proteins to support cell culture. For example, previous studies showed that tropoelastin immobilised PAC surface enhanced endothelial cell growth up to five days,[29] and fibronectin immobilised PAC surface enhanced primary osteoblast growth up to 14 days.[45] Future extension of this method to even higher throughput plate formats, such as 1536-well plates, also has the potential to facilitate high-throughput screening (HTS) assays in drug development. However, edge effects could potentially decrease homogeneity of biomolecule immobilisation across the well on higher

throughput plates and would need further optimisation. Ultimately, plasma activation of microplates will allow for a faster and more convenient platform to study biological processes with user selected biomolecules.

Acknowledgement

Supporting Information Available

The following files are available for download. Supporting Information: Additional data including deconvolusion of C1s peaks of PIII/PAC treated microplates, FTIR-ATR of PIII/PAC treated microplates, EPR spectrum of PIII/PAC treated PS sheets, absorbance spectra of PIII/PAC treated microplates, normalised absorbance of PIII/PAC treated microplates, fluorescence spectra of low nitrogen PAC, DNA immobilised low nitrogen PAC and streptavidin immobilised low nitrogen PAC, relative immobilised DNA density, and further optimised DNA hybridisation results.

References

(1) Butler, J. E. Solid Supports in Enzyme-Linked Immunosorbent Assay and Other SolidPhase Immunoassays. *Methods* **2000**, *22*, 4–23.

(2) Engvall, E.; Perlmann, P. Enzyme-linked immunosorbent assay (ELISA) quantitative assay of immunoglobulin G. *Immunochemistry* **1971**, *8*, 871–874.

(3) Lequin, R. M. Enzyme immunoassay (EIA)/enzyme-linked immunosorbent assay (ELISA). *Clinical Chemistry* **2005**, *51*, 2415–2418.

(4) Zhang, Z.-R.; Hughes, M. D.; Morgan, L. J.; Santos, A. F.; Hine, A. V. Fluorescent microplate-based analysis of protein-DNA interactions II: immobilized DNA. 2018; https://www.future-science.com/doi/abs/10.2144/03355st07, Archive Location: London, UK Publisher: Future Science Ltd London, UK.

(5) Desbordes, S. C.; Studer, L. Adapting human pluripotent stem cells to high-throughput and high-content screening. *Nature Protocols* **2013**, *8*, 111–130, Number: 1 Publisher: Nature Publishing Group.

(6) Barker, S. L.; LaRocca, P. J. Method of production and control of a commercial tissue culture surface. *Journal of tissue culture methods* **1994**, *16*, 151–153.

(7) Gharaibeh, B.; Lu, A.; Tebbets, J.; Zheng, B.; Feduska, J.; Crisan, M.; P´eault, B.; Cummins, J.; Huard, J. Isolation of a slowly adhering cell fraction containing stem cells from murine skeletal muscle by the preplate technique. *Nature Protocols* **2008**, *3*, 1501–1509, Number: 9 Publisher: Nature Publishing Group.

(8) Nagaoka, M.; Koshimizu, U.; Yuasa, S.; Hattori, F.; Chen, H.; Tanaka, T.; Okabe, M.; Fukuda, K.; Akaike, T. E-Cadherin-Coated Plates Maintain Pluripotent ES Cells

without Colony Formation. *PLOS ONE* **2006**, *1*, e15, Publisher: Public Library of Science.

(9)   Nimse, S. B.; Song, K.; Sonawane, M. D.; Sayyed, D. R.; Kim, T. Immobilization Techniques for Microarray: Challenges and Applications. *Sensors* **2014**, *14*, 22208– 22229, Number: 12 Publisher: Multidisciplinary Digital Publishing Institute.

(10) Dugas, V.; Depret, G.; Chevalier, Y.; Nesme, X.; Souteyrand, Immobilization of singlestranded DNA fragments to solid surfaces and their repeatable specific hybridization: covalent binding or adsorption? *Sensors and Actuators B: Chemical* **2004**, *101*, 112– 121.

(11) Butler, J. E.; Ni, L.; Brown, W. R.; Joshi, K. S.; Chang, J.; Rosenberg, B.; Voss, E. W.
The immunochemistry of sandwich elisas—VI. Greater than 90% of monoclonal and 75% of polyclonal anti-fluorescyl capture antibodies (CAbs) are denatured by passive adsorption. *Molecular Immunology* **1993**, *30*, 1165–1175.

(12) Yousefi, H.; Su, H.-M.; Ali, M.; Filipe, C. D. M.; Didar, T. F. Producing Covalent Microarrays of Amine-Conjugated DNA Probes on Various Functional Surfaces to Create Stable and Reliable Biosensors. *Advanced Materials Interfaces* **2018**, *5*, 1800659, eprint: https://onlinelibrary.wiley.com/doi/pdf/10.1002/admi.201800659.

(13) Vroman, L.; Adams, A. L. Findings with the recording ellipsometer suggesting rapid exchange of specific plasma proteins at liquid/solid interfaces. *Surface Science* **1969**, *16*, 438–446.

(14) Kaur, J.; Singh, K. V.; Raje, M.; Varshney, G. C.; Suri, C. R. Strategies for direct attachment of hapten to a polystyrene support for applications in enzyme-linked immunosorbent assay (ELISA). *Analytica Chimica Acta* **2004**, *506*, 133–135.

(15) Chrisey, L. Covalent attachment of synthetic DNA to self-assembled monolayer films. *Nucleic Acids Research* **1996**, *24*, 3031–3039.

(16) Rogers, Y.-H.; Jiang-Baucom, P.; Huang, Z.-J.; Bogdanov, V.; Anderson, S.; Boyce-Jacino, M. T. Immobilization of Oligonucleotides onto a Glass Support via Disulfide Bonds: A Method for Preparation of DNA Microarrays. *Analytical Biochemistry* **1999**, *266*, 23–30.

(17) O'Donnell, M. J.; Tang, K.; K¨oster, H.; Smith, C. L.; Cantor, C. R. High-Density, Covalent Attachment of DNA to Silicon Wafers for Analysis by MALDI-TOF Mass Spectrometry. *Analytical Chemistry* **1997**, *69*, 2438–2443.

(18) Rehman, F. N.; Audeh, M.; Abrams, E. S.; Hammond, P. W.; Kenney, M.; Boles, T. C.
Immobilization of acrylamide-modified oligonucleotides by co-polymerization. *Nucleic Acids Research* **1999**, *27*, 649–655.

(19) Zhang, Y.; Li, L.; Yu, C.; Hei, T. Chitosan-coated polystyrene microplate for covalent immobilization of enzyme. *Analytical and Bioanalytical Chemistry* **2011**, *401*, 2311–2317.

(20) Hoffmann, C.; Pinelo, M.; Woodley, J. M.; Daugaard, A. E. Development of a thiol-ene based screening platform for enzyme immobilization demonstrated using horseradish peroxidase. *Biotechnology Progress* **2017**, *33*, 1267–1277.

(21) Jeon, B.-J.; Kim, M.-H.; Pyun, J.-C. Parylene-A coated microplate for covalent immobilization of proteins and peptides. *Journal of Immunological Methods* **2010**, *353*, 44–48.

(22) Yoo, G.; Park, M.; Lee, E.-H.; Jose, J.; Pyun, J.-C. Immobilization of E. coli with autodisplayed Z-domains to a surface-modified microplate for immunoassay. *Analytica Chimica Acta* **2011**, *707*, 142–147.

(23) Wang, S.; Wen, S.; Shen, M.; Guo, R.; Cao, X.; Wang, J.; Shi, X. Aminopropyltriethoxysilane-mediated surface functionalization of hydroxyapatite nanoparticles: synthesis, characterization, and in vitro toxicity assay. *International Journal of Nanomedicine* **2011**, *6*, 3449–3459.

(24) Bilek, M. M.; McKenzie, D. R. Plasma modified surfaces for covalent immobilization of functional biomolecules in the absence of chemical linkers: towards better biosensors and a new generation of medical implants. *Biophysical Reviews* **2010**, *2*, 55–65.

(25) Nosworthy, N. J.; Ho, J. P. Y.; Kondyurin, A.; McKenzie, D. R.; Bilek, M. M. M. The attachment of catalase and poly-l-lysine to plasma immersion ion implantation-treated polyethylene. *Acta Biomaterialia* **2007**, *3*, 695–704.

(26) Kosobrodova, E.; Gan, W. J.; Kondyurin, A.; Thorn, P.; Bilek, M. M. M. Improved Multiprotein Microcontact Printing on Plasma Immersion Ion Implanted Polystyrene. *ACS Applied Materials & Interfaces* **2018**, *10*, 227–237.

(27) Yin, Y.; Fisher, K.; Nosworthy, N. J.; Bax, D.; Rubanov, S.; Gong, B.; Weiss, A. S.; McKenzie, D. R.; Bilek, M. M. M. Covalently Bound Biomimetic Layers on Plasma Polymers with Graded Metallic Interfaces for in vivo Implants. *Plasma Processes and Polymers* **2009**, *6*, 658–666.

(28) Gan, B. K.; Kondyurin, A.; Bilek, M. M. M. Comparison of protein surface attachment on untreated and plasma immersion ion implantation treated polystyrene: protein

islands and carpet. *Langmuir: the ACS journal of surfaces and colloids* **2007**, *23*, 2741–2746.

(29) Waterhouse, A.; Yin, Y.; Wise, S. G.; Bax, D. V.; McKenzie, D. R.; Bilek, M. M.; Weiss, A. S.; Ng, M. K. The immobilization of recombinant human tropoelastin on metals using a plasma-activated coating to improve the biocompatibility of coronary stents. *Biomaterials* **2010**, *31*, 8332–8340.

(30) Tran, C. T. H.; Craggs, M.; Smith, L. M.; Stanley, K.; Kondyurin, A.; Bilek, M. M.; McKenzie, D. R. Covalent linker-free immobilization of conjugatable oligonucleotides on polypropylene surfaces. *RSC Advances* **2016**, *6*, 83328–83336.

(31) Kosobrodova, E.; Mohamed, A.; Su, Y.; Kondyurin, A.; dos Remedios, C. G.; McKenzie, D. R.; Bilek, M. M. M. Cluster of differentiation antibody microarrays on plasma immersion ion implanted polycarbonate. *Materials Science and Engineering: C* **2014**, *35*, 434–440.

(32) Bilek, M. M. M.; Bax, D. V.; Kondyurin, A.; Yin, Y.; Nosworthy, N. J.; Fisher, K.; Waterhouse, A.; Weiss, A. S.; dos Remedios, C. G.; McKenzie, D. R. Free radical functionalization of surfaces to prevent adverse responses to biomedical devices. *Proceedings of the National Academy of Sciences of the United States of America* **2011**, *108*, 14405–14410.

(33) North, S. H.; Lock, E. H.; Cooper, C. J.; Franek, J. B.; Taitt, C. R.; Walton, S. G. Plasma-Based Surface Modification of Polystyrene Microtiter Plates for Covalent Immobilization of Biomolecules. *ACS Applied Materials & Interfaces* **2010**, *2*, 2884–2891, Publisher: American Chemical Society.

(34) Boulares-Pender, A.; Prager-Duschke, A.; Elsner, C.; Buchmeiser, M. R. Surfacefunctionalization of plasma-treated polystyrene by hyperbranched polymers

and use in biological applications. *Journal of Applied Polymer Science* **2009**, *112*, 2701–2709.

(35) O'Sullivan, D.; O'Neill, L.; Bourke, P. Direct Plasma Deposition of Collagen on 96-Well

Polystyrene Plates for Cell Culture. *ACS Omega* **2020**, *5*, 25069–25076.

(36) Ham, H. O.; Liu, Z.; Lau, K. H. A.; Lee, H.; Messersmith, P. B. Facile DNA Immobilization on Surfaces through a Catecholamine Polymer. *Angewandte Chemie International Edition* **2011**, *50*, 732–736, eprint:

https://onlinelibrary.wiley.com/doi/pdf/10.1002/anie.201005001.

(37) V¨alimaa, L.; Pettersson, K.; Vehnia¨inen, M.; Karp, M.; L¨ovgren, T. A High-Capacity Streptavidin-Coated Microtitration Plate. *Bioconjugate Chemistry* **2003**, *14*, 103–111, Publisher: American Chemical Society.

(38) Gan, B.; Bilek, M.; Kondyurin, A.; Mizuno, K.; McKenzie, D. Etching and structural changes in nitrogen plasma immersion ion implanted polystyrene films. *Nuclear Instruments and Methods in Physics Research Section B: Beam Interactions with Materials and Atoms* **2006**, *247*, 254–260.

(39) Sharifahmadian, O.; Zhai, C.; Hung, J.; Shineh, G.; Stewart, C. A.; Fadzil, A. A.; Ionescu, M.; Gan, Y.; Wise, S. G.; Akhavan, B. Mechanically robust nitrogen-rich plasma polymers: Biofunctional interfaces for surface engineering of biomedical implants. *Materials Today Advances* **2021**, *12*, 100188.

(40) Kosobrodova, E.; Kondyurin, A.; McKenzie, D. R.; Bilek, M. M. M. Kinetics of post-treatment structural transformations of nitrogen plasma ion immersion implanted polystyrene. *Nuclear Instruments and Methods in Physics Research Section B: Beam Interactions with Materials and Atoms* **2013**, *304*, 57–66.

(41) Kondyurin, A. V.; Bilek, M. *Ion beam treatment of polymers: application aspects from medicine to space*, 2nd ed.; Elsevier: Amsterdam, Netherlands, 2015.

(42) Kosobrodova, E. Free radical kinetics in a plasma immersion ion implanted polystyrene: Theory and experiment. *Nuclear Instruments and Methods in Physics Research Section B: Beam Interactions with Materials and Atoms* **2012**, *280*, 26–35.

(43) Yin, Y.; Bilek, M. M.; McKenzie, D. R.; Nosworthy, N. J.; Kondyurin, A.; Youssef, H.; Byrom, M. J.; Yang, W. Acetylene plasma polymerized surfaces for covalent immobilization of dense bioactive protein monolayers. *Surface and Coatings Technology* **2009**, *203*, 1310–1316.

(44) Santos, M.; Filipe, E. C.; Michael, P. L.; Hung, J.; Wise, S. G.; Bilek, M. M. M. Mechanically Robust Plasma-Activated Interfaces Optimized for Vascular Stent Applications.
ACS Applied Materials & Interfaces **2016**, *8*, 9635–9650.

(45) Akhavan, B.; Croes, M.; Wise, S. G.; Zhai, C.; Hung, J.; Stewart, C.; Ionescu, M.; Weinans, H.; Gan, Y.; Amin Yavari, S.; Bilek, M. M. Radical-functionalized plasma polymers: Stable biomimetic interfaces for bone implant applications. *Applied Materials Today* **2019**, *16*, 456–473.

(46) Kondyurin, A.; Naseri, P.; Fisher, K.; McKenzie, D. R.; Bilek, M. M. Mechanisms for surface energy changes observed in plasma immersion ion implanted polyethylene: The roles of free radicals and oxygen-containing groups. *Polymer Degradation and Stability* **2009**, *94*, 638–646.

(47) Yeo, G. C.; Kondyurin, A.; Kosobrodova, E.; Weiss, A. S.; Bilek, M. M. M. A sterilizable, biocompatible, tropoelastin surface coating immobilized by energetic ion activation. *Journal of The Royal Society Interface* **2017**, *14*, 20160837.

(48) Shadpour, H.; Musyimi, H.; Chen, J.; Soper, S. A. Physiochemical properties of various polymer substrates and their effects on microchip electrophoresis performance. *Journal of Chromatography A* **2006**, *1111*, 238–251.

(49) Auld, D. S.; Coassin, P. A.; Coussens, N. P.; Hensley, P.; Klumpp-Thomas, C.;
Michael, S.; Sittampalam, G. S.; Trask, O. J.; Wagner, B. K.; Weidner, J. R.;
Wildey, M. J.; Dahlin, J. L. In *Assay Guidance Manual*; Markossian, S. et al. , Eds.;
Eli Lilly & Company and the National Center for Advancing Translational Sciences:
Bethesda (MD), 2004.

(50) Tran, C. T.; Kondyurin, A.; Chrzanowski, W.; Bilek, M. M.; McKenzie, D. R. Influence of pH on yeast immobilization on polystyrene surfaces modified by energetic ion bombardment. *Colloids and Surfaces B: Biointerfaces* **2013**, *104*, 145–152.

(51) Kushalkar, M. P.; Liu, B.; Liu, J. Promoting DNA Adsorption by Acids and Polyvalent Cations: Beyond Charge Screening. *Langmuir* **2020**, *36*, 11183–11195.

(52) Saenger, W. *Principles of Nucleic Acid Structure*; Springer Science & Business Media,
2013; Google-Books-ID: gaoJCAAAQBAJ.

(53) Cholko, T.; Kaushik, S.; A. Chang, C.-e. Dynamics and molecular interactions of singlestranded DNA in nucleic acid biosensors with varied surface properties. *Physical Chemistry Chemical Physics* **2019**, *21*, 16367–16380, Publisher: Royal Society of Chemistry.

(54) van Oss, C. J.; Giese, R. F.; Bronson, P. M.; Docoslis, A.; Edwards, P.; Ruyechan, W. T. Macroscopic-scale surface properties of streptavidin and their influence on aspecific interactions between streptavidin and dissolved biopolymers. *Colloids and Surfaces B: Biointerfaces* **2003**, *30*, 25–36.

(55) Phillips, M. F.; Lockett, M. R.; Rodesch, M. J.; Shortreed, M. R.; Cerrina, F.; Smith, L. M. In situ oligonucleotide synthesis on carbon materials: stable substrates for microarray fabrication. *Nucleic Acids Research* **2007**, *36*, e7–e7.

(56) Jin, L.; Horgan, A.; Levicky, R. Preparation of End-Tethered DNA Monolayers on Siliceous Surfaces Using Heterobifunctional Cross-Linkers. *Langmuir* **2003**, *19*, 6968–6975.